

**NOAA NESDIS
CENTER for SATELLITE APPLICATIONS and
RESEARCH**

**GOES-R Advanced Baseline Imager
(ABI) Algorithm Theoretical Basis
Document For
Ocean Dynamics**

EileenMaturi, NOAA/NESDIS/STAR

Version 1.0

September 3, 2010

THIS PAGE IS INTENTIONALLY LEFT BLANK

Table of contents

LIST OF ACRONYMS	1
1 INTRODUCTION	5
1.1 Purpose of this document	5
1.2 Who should use this document.....	5
1.3 Inside each section.....	5
1.4 Related Documents.....	5
1.5 Revision history	5
2 OBSERVING SYSTEM OVERVIEW	6
2.1 Products Generated.....	6
2.2 Instrument Characteristics	7
3 ALGORITHM DESCRIPTION	10
3.1 Algorithm Overview	10
3.2 Processing Outline	10
3.3 Algorithm Input	12
3.3.1 Primary Sensor Data	13
3.3.2 Ancillary Data	13
3.3.3 Derived data	13
3.4 Theoretical Description.....	14
3.4.1 Physics of the Problem.....	14
3.4.2 Mathematical Description.....	17
3.5 Algorithm Output.....	20
3.6 Product Quality.....	20
3.6.1 Quality flags.....	20
3.6.2 Product Quality Information	21
3.7 Metadata.....	21
3.7.1 File Level Metadata summarizing the contents of the data file.....	21
3.7.2 Product specific metadata for Ocean Dynamics (separately for oceans and offshore oceans).....	22
4 TEST DATA SETS AND OUTPUTS	22

4.1	<i>GOES-R Proxy Input Data Sets</i>	23
4.1.1	SEVIRI Data	23
4.2	Output from Proxy Data Sets	24
4.2.1	SEVIRI Brightness Temperatures	24
4.3	Precision and Accuracy Estimates	25
4.3.1	Validation against NCOM	26
5	PRACTICAL CONSIDERATIONS	29
5.1	Numerical Computation Considerations.....	29
5.2	Programming and Procedural Considerations	29
5.3	Quality Assessment and Diagnostics	30
5.3.1	Exception Handling	30
5.3.2	Validation	31
6	ASSUMPTIONS AND LIMITATIONS.....	33
6.1	Performance	33
6.2	Assumed Sensor Performance	34
6.3	Pre-Planned Product Improvements	34
7	REFERENCES	34

LIST OF ACRONYMS

ABI – Advanced Baseline Imager
AIT – Algorithm Integration Team
AQC - Automatic Quality Control
ASCII - American Standard Code for Information Interchange
ATBD – Algorithm Theoretical Basis Document
AVHRR - Advanced Very High Resolution Radiometer
AWG – Algorithm Working Group
CC – Cross Correlation
CONUS – Continental United States
CRTM – Community Radiative Transfer Model
CTP – Cloud-top Pressure
NWP – Numerical Weather Prediction
DMW – Derived Motion Winds
DMWA – Derived Motion Winds Algorithm
EE – Expected Error
EEZ – Exclusive Economic Zone
EUMETSAT - European Organization for the Exploitation of Meteorological Satellites.
FD – Full Disk
F&PS – Functional and Performance Specification
GFS – Global Forecast System
GOES – Geostationary Operational Environmental Satellite
GPO – GOES-R Program Office
IGFOV – Instantaneous Geometric Field of View
INR – Image Navigation and Registration
IO – Input/Output
IR – Infrared
LSB – Least Significant Bit
LWIR – Longwave Infrared
MRD – Mission Requirements Document
MSB – Most Significant Bit
MSG – Meteosat Second Generation

MODIS - Moderate Resolution Imaging Spectroradiometer
MVD – Mean Vector Difference
MSFC – Marshall Space Flight Center
NASA – National Aeronautics and Space Administration
NCSA – National Center for Super Computing Applications
NCEP – National Centers for Environmental Prediction
NESDIS – National Environmental Satellite, Data, and Information Service
NOAA – National Oceanic and Atmospheric Administration
NWP – Numerical Weather Prediction
OSDPD – Office of Satellite Data Processing and Distribution
ODPA - Ocean Dynamics Product Algorithm
PDF – Probability Distribution Function
PG – Product Generation
PORD – Performance Operational Requirements Document
QC – Quality Control
QI – Quality Indicator
RAOB – Radiosonde Observation
RMSE – Root Mean Square Error
SD – Standard Deviation
SEVIRI – Spinning Enhanced Visible Infrared Imager
SOI – Successive Order of Interaction
SSD – Sum of Squared Differences
STAR – Center for Satellite Applications and Research
SWIR – Shortwave Infrared
TELL – Tracking Error Lower Limit
TOA – Top of Atmosphere
TRR – Test Readiness Review
VAGL - Vendor Allocated Ground Latency
VIS – Visible
WRF – Weather Research and Forecasting

LIST OF FIGURES

Figure 1: High level flowchart of the ABI ocean dynamics product algorithms (note: SST data are not used at present). *SSD = sum of squared differences	12
Figure 2: An example of the output of the SSD algorithm applied to Meteosat-8 data	19
Figure 3: Full disk 0.63, 0.86 and 11 μm false color image from SEVIRI for 2 UTC on 4 Aug 2006	24
Figure 4: Example vector output from Ocean Dynamic Algorithm derived from Meteosat-8 SEVIRI image triplet centered at 12 UTC on July 8, 2005	25
Figure 5: An example of the output from the US Navy NCOM Model	26
Figure 6: The distribution of the Ocean Dynamics Algorithm-NCOM vector component differences	27
Figure 7: The geographical distribution of the vector component differences.....	27
Figure 8: Illustrates the relationship between strength of the gradient within the target window and the vector component difference.	28
Figure 9: Surface Current Field of the Northwest Atlantic from Real-Time Ocean Forecast System. Note the erroneous position of the core of the Gulf Stream.	31
Figure 10: Example of the surface current field from the Ocean Surface current Analyses-Real time, available from NOAA/NESDIS. Note the coarse spatial resolution, and the inability to derive currents within 100 km of the coastline.	32
Figure 11: Example of ocean surface currents from CODAR off of California	33

LIST OF TABLES

Table 1: F&PS requirements for the Ocean Dynamics Product for Ocean Currents.....	6
Table 2: F&PS requirements for the Ocean Dynamics Product for Ocean Currents (OFFSHORE)...	7
Table 3: Summary of the current ABI Channel Numbers and Wavelengths	8
Table 4: Image navigation and registration pre-launch specification (3σ) for day and night for GOES 8-12, GOES 13/0/P, and GOES-R series of satellites. The actual computed image navigation and registration performance statistics for GOES-12 and 13 are in brackets.(Computed values courtesy of G. Jedlovec; NASA/MSFC).....	9
Table 5: Quality flag word bit definitions	21
Table 6: SEVIRI channels serving as GOES-R ABI proxy data for the GOES-R ODAP.....	23
Table 7: Seasonal variation of retrieval accuracy for vectors derived from well-defined features	29

1 INTRODUCTION

1.1 Purpose of this document

The purpose of this document is to describe the algorithm developed to generate the GOES-R ocean dynamic (OD) product using the GOES-R Advanced Baseline Algorithm (ABI) observations. It will provide information to maintain and modify the algorithm.

1.2 Who should use this document

The intended user of this document are those interested in understanding the physical basis of the algorithms and how to use the output of this algorithm to optimize the OD product for a particular application. This document also provides information useful to anyone maintaining, modifying, or improving the original algorithm.

1.3 Inside each section

This document is broken down into the following main sections:

- **System Overview:** Provides relevant details of the ABI and provides a brief description of the products generated by the algorithms.
- **Algorithm Description:** Provides all the detailed description of the algorithm including its physical basis, its input and its output, performance estimates and some practical considerations.
- **Assumptions and Limitations:** Provides an overview of the current limitations of the approach and gives the plan for overcoming these limitations with further algorithm development.

1.4 Related Documents

This document relates to the GOES-R Mission Requirements Document (MRD) and to the references given throughout. This document currently does not relate to any other document outside of the specifications of the GOES-R Ground Segment Functional and Performance Specification (F&PS) and to the references given throughout.

1.5 Revision history

Version 0.0 was created by Dr Tim Mavor, with the intent to accompany the delivery of the version 0.0 algorithms to the GOES-R AWG Algorithm Integration Team (AIT). (July 2008).

This version was created by Eileen Maturi, Igor Appel and Andy Harris, to meet 80% ATBD requirement. (July 2010)

2 OBSERVING SYSTEM OVERVIEW

This section will describe the products generated by the GOES-R ABI Ocean Dynamics Product Algorithm (ODPA) and the requirements it places on the sensor.

2.1 Products Generated

The GOES-R ABI Ocean Dynamics Products Algorithm employs a sequence of a single spectral band images to derive the Ocean Dynamics product. These images will be used to track ocean motion in cloud free areas over time, either directly using the ABI bands designated in Table 3.

The algorithm will utilize the ABI data, to derive an ocean motion. The ODPA will generate products over the various ABI Full Disk (FD), Continental United States (CONUS), and mesoscale scans.

Currently, ODPA employs a sequence of ABI images to estimate ocean motion for a set of targeted tracers in cloud-free areas. Later modifications will implement this validated approach to a regular grid providing ocean motion to each pixel of ABI observations.

Table 1 and Table 2 outlines the specifications for the GOES-R Ocean Dynamics products as defined in the latest version of the GOES-R Ground Segment Project Functional and Performance Specification (F&PS) requirements document.

Ocean Currents	Threshold
Primary instrument	ABI
Prioritization Tier	III
Geographic Coverage Conditions	Full Disk/Mesoscale
Vertical Resolution	Surface
Horizontal Resolution	2KM
Measurement Accuracy	1km/hr(0.3m/sec) in both meridional and zonal directions
Measurement Precision	1km/hr(0.3m/sec) in both meridional and zonal directions
Refresh rate/coverage time	6 hrs

Table 1: F&PS requirements for the Ocean Dynamics Product for Ocean Currents

Ocean Currents (OFFSHORE)	Threshold
Primary instrument	ABI
Prioritization Tier	III
Geographic Coverage Conditions	U.S. EEZ Waters/Mesoscale
Vertical Resolution	Surface
Horizontal Resolution	2KM
Measurement Accuracy	1km/hr(0.3m/sec) in both meridional and zonal directions
Measurement Precision	1km/hr(0.3m/sec) in both meridional and zonal directions
Refresh rate/coverage time	3 hrs

Table 2: F&PS requirements for the Ocean Dynamics Product for Ocean Currents (OFFSHORE)

2.2 Instrument Characteristics

The GOES-R ABI has been designed to address the needs of many users of geostationary data and products (*Schmit, et al, 2005*) It will offer more spectral bands (to enable new and improved products), higher spatial resolution (to better monitor small-scale features), and faster imaging (to improve temporal sampling and to scan additional regions) than the current GOES imager. The spatial resolution of the ABI data will be nominally 2 km for the infrared bands and 0.5 km for the 0.64- μm visible band. Table 3 provides a summary of the 16 spectral bands that will be available on the ABI and their intended uses. The final channel set for use to monitor ocean motion will be determined later. The channels that are expected to be tested for use in Ocean Dynamics algorithm include 7, 13, 14 and 15. When the OD algorithm is based upon a derived product (SST), good absolute accuracy is required for the bands necessary for SST retrieval.

<i>Channel Number</i>	<i>Central Wavelength (μm)</i>	<i>Nominal sub satellite IGFOV (km)</i>	<i>Used in Ocean Dynamics</i>
1	0.47	1	
2	0.64	0.5	
3	0.86	1	
4	1.38	2	
5	1.61	1	
6	2.26	2	
7	3.9	2	
8	6.15	2	
9	7.0	2	
10	7.74	2	
11	8.5	2	
12	9.7	2	
13	10.35	2	
14	11.2	2	√
15	12.3	2	
16	1.3	2	

Table 3: Summary of the current ABI Channel Numbers and Wavelengths

To determine ocean motion, the Ocean Dynamics algorithm compares values of SST or brightness temperatures for pairs of images. Because ocean motion is slow in comparison with the atmosphere, significant improvements in the performance of the image navigation and registration, expected with GOES-R and improving the retrieval of ocean motion, is critically important. The stability of the frame-to-frame navigation, in particular, is a key factor for deriving accurate ocean motion vectors. Table 4 copied from GOES-R ATBD for Derived Motion Wind) shows the image navigation and registration pre-launch specifications (3σ) in black for the GOES-8-12, GOES-13/O/P, and GOES-R series of satellites.

	GOES 8-12	GOES 13, O, P	GOES-R
	Day/Night	Day/Night	
Absolute	4.0/6.0	2.3	1.0/1.5
Navigation (km)	(4.5 / 5.0)		
Within Image (km)	1.6/1.6	2.0	1.0
Image to Image (km)			
	--	--	0.75
5-7 Minutes	(2.3 / 2.3)	(0.6/0.6)	1.0
	1.5 / 2.5	1.3	0.75
15 min	(2.8 / 3.2)	(1.0/1.3)	1.0
	3.0 / 3.8	1.8	0.75
90 min			1.0
24 hr	6.0 / 6.0	4.0	24 hr

Table 4: Image navigation and registration pre-launch specification (3σ) for day and night for GOES 8-12, GOES 13/O/P, and GOES-R series of satellites. The actual computed image navigation and registration performance statistics for GOES-12 and 13 are in brackets. (Computed values courtesy of G. Jedlovec; NASA/MSFC)

The actual computed image navigation and registration performance statistics for GOES-12 (using four 1-week periods of residual data from 2005 and 2006) and for GOES-13 (using two days from special collection period in December 2006) based on the standard deviation of the residual differences calculated from satellite image navigation and registration (INR) data. It is clear from this table that the image navigation and registration performance has improved with each new series of GOES satellites. The GOES-13 image-to-image registration accuracy, for example, is substantially improved over its predecessors and approaches the GOES-R specifications, which represent even a further improvement. Higher spatial, spectral, and temporal resolution, together with increased radiometric performance and improved navigation/registration performance of the GOES-R ABI is expected to result in better target selection and improved feature tracking.

3 ALGORITHM DESCRIPTION

A complete description of the algorithm at the current level of maturity (which will improve with each revision) is provided in this section that includes an overview, processing outline, the physics of the problem, mathematical description, input and output.

3.1 Algorithm Overview

The ODP developed for the GOES-R ABI instrument has its heritage with the Atmosphere Motion Vectors algorithm being used operationally today at NOAA/NESDIS for the present series of GOES satellites (*Breaker et al, 2005; Castelao et al, 2005, 2006*). The Ocean Dynamics algorithm is based upon the Sum of Squared Distances (SSD) Method that the Derived Wind Product Algorithm (DWPA) has also used at NOAA/NESDIS for deriving Atmospheric Motion Vectors (GOES-R ABI Derived Motion Winds ATBD; *Merrill et al, 1989, 1991; Nieman et al, 1997, Velden et al, 2005*).

The following steps are carried out in the process of generating the Ocean Dynamics product:

1. Collect three consecutive calibrated, navigated, and co-registered images for the same area of observations in predetermined spectral channels;
2. Locate and select a suitable cloud free targets in the second image (middle image; time= t_0) of image triplet;
3. Use a pattern matching algorithm to locate the cloud free targets in an earlier and later image;
4. Compute corresponding displacement vectors for the targets from their original locations for each image pair of the triplets;
5. Compute mean vector displacement (average from speeds derived for each pair) valid at time = t_0 ;
6. Perform quality assurance on ocean motion vectors. Flag suspect vectors. Compute and append quality indicators to each vector. If the quality of the vectors is poor, then the vectors are removed from the output and are not included in the results.

3.2 Processing Outline

The Ocean Dynamics algorithm works in a multi-stage process using a sequence of three images separated by 3 hours following the requirements formulated in specifications. Currently it is assumed that equal in size GOES-R images include the same set of navigated and co-registered pixels.

A two-dimensional first derivative operator is applied to the cloud free areas of the middle image to highlight ocean surface regions with high first spatial derivatives, used as targeted features. The location of targets including high gradient magnitude in the image is tracked to traceable features between two pairs of images in an image triplet to estimate ocean motion vectors. Mean vector displacement between two vectors derived from two pairs of images is included in output after careful quality control.

The processing outline of the ODP is summarized in **Error! Reference source not found..** The

Algorithm could be run on data consisting of either GOES-R SST or brightness temperature from relevant ABI bands for the ODP.

To optimize calculations processes, the algorithm is designed to run on segments of data consisting of multiple scan lines. Processing begins only after a data “buffer,” including three times more scan lines than target size, has been filled in the sequence with line segment data from all three images as well as cloud masks. Suitable targets are selected from the middle image buffer only, while vector processing is limited to the middle portion of the buffer to allow for north-south displacements of the image features.

Once the data buffer is full, the middle image portion of the buffered segment is divided into small, square (in pixel space) target boxes and each box is processed as a potential tracer. Within each box the algorithm locates the strongest 2-D gradient in the brightness temperature field (or SST) and re-centers the box on this location. A brightness temperature gradient threshold is used to prevent target selection on very weak gradients. This test eliminates targets that lack the gradients necessary to track motion reliably.

If a potential tracer makes it through the target quality control, a search region much larger than the target size (in pixel space) is defined in each of two non-target images. The algorithm then searches all possible pixel configurations (scenes) within this region for acceptable matches to the target scene. The scene that minimizes the sum of squares difference between the target and search windows is accepted as the best match. Two sub-vectors are generated in the tracking process, one vector for the backward time step and one vector for the forward time step. Acceptable matches must exceed a minimum correlation threshold, and accelerations between sub-vectors exceeding a user defined threshold are not permitted (vectors are discarded).

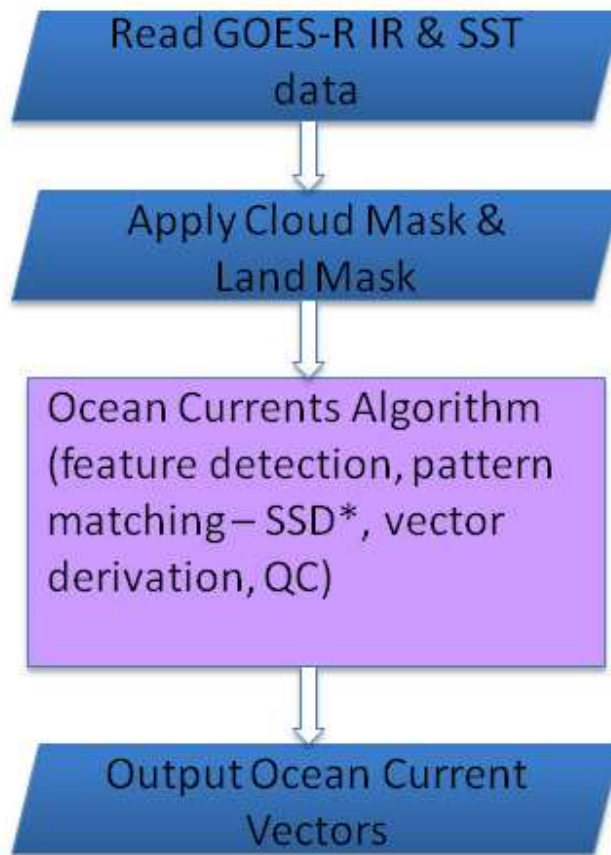


Figure 1: High level flowchart of the ABI ocean dynamics product algorithms (note: SST data are not used at present). *SSD = sum of squared differences

The ocean motion vectors will have several dependencies that will affect the accuracy and precision of the product. As the product will be based upon sequential clear views of the ocean surface, consistent image navigation from scene to scene is essential to optimize the interpretation of such motion as being advective processes occurring on the ocean surfaces. Another dependency issue is that of the cloud-mask. While the input ocean scene will need to be devoid of clouds in order to avoid the tracking of such regions in sequential images, many dynamically active regions of the ocean (strong gradient regions, upwelling zones, eddies) could be erroneously flagged as clouds. The transient nature of such events is of particular importance to the oceanographic community; hence inclusion of such features in the Ocean Dynamics product is essential. Lastly, while highly accurate and precise SST or brightness temperature fields are always desirable, it is the image-to-image consistency that is essential including the treatment of diurnal warming events, and any daytime versus nighttime bias.

3.3 Algorithm Input

This section describes the input needed to process the ODPA. While the ODPA uses information at the pixel level (e.g., cloud mask, brightness temperature or SST), the derived products are currently representative of a group of pixels (a target box). The following sections describe the

actual input needed to run the ODP.

The algorithm is designed to process information only after a data buffer has been filled with data from all three images in the tracking sequence. The buffer is necessary to capture the motion of features up or down in the image and to take into account varying in time configuration of cloud mask. The consideration of cloud masks for the first and the third images is a characteristic property of Ocean Dynamics principally distinguishing it from the algorithms used for wind retrievals. Once the buffer is full, the algorithm processes only the middle portion of the buffer (typically lines 31 – 45) for suitable tracers. Processing proceeds from west to east until the earth edge is encountered or no more elements exist in the line segment. After processing is completed over the middle portion of the buffer, data is then shifted “up” (lines 16 – 30 copied into lines 1 – 15) and new data is added to the bottom of the buffer. The process is repeated until the number of lines remaining in the line segment is smaller than the size of a target scene. At this point the extra lines are simply saved in the buffer and control is returned to the framework until the next line segment is read into memory. The following sections describe the actual input needed to run the ODAP.

3.3.1 Primary Sensor Data

The list below contains the primary sensor data used by the ODAP. By primary sensor data, we mean information that is derived solely from the ABI observations and geolocation information.

- Calibrated and navigated brightness temperatures for ABI channel 14 (or other SST-sensitive channels) for three consecutive images.

3.3.2 Ancillary Data

The following describes the ancillary data required to run the ODAP. By ancillary data, we mean data not included in the ABI observations or geolocation data.

- **Land/water mask**

A global pixel level land/water mask. Currently the mask is provided within GEOCAT. It will be included in the AIT Framework data structures.

3.3.3 Derived data

This section describes the data that must be derived before the ODAP is executed. The following output of upstream cloud product algorithms from the GOES-R AWG cloud team is used in the Ocean Dynamics derivation process.

- **Cloud Mask**

The ODPa requires three sets of image pixel level Cloud Masks for each image of a triplet. These are used to estimate where clear sky is located. The cloud mask is analyzed when selecting which target scenes to process.

- **Sea Surface Temperature** (not used at present)

The sea surface temperature is another candidate derived field which could be used by the ODPa. However, the noise introduced by the retrieval algorithm can cause problems with the pattern matching process. While there is a benefit in ensuring that absolute differences between temperatures in image pairs are minimized, the change in atmospheric correction over a period of 3 hours is deemed of less significance than the impact of the aforementioned introduction of noise in the temperature pattern.

3.4 Theoretical Description

Ocean motion detection is the process of determining the displacement of water pixels. It always involves assumptions of the radiometric characteristics of water, particularly those that relate to the brightness temperature in the 11 micron band. In the ODPa, a target area in one image is compared with many areas of the same size in a search region of the previous and following images. The displacement of water is then defined by the location in the images where the sum-of-squared-differences between brightness temperatures (or SST) is the smallest. This approach makes the basic assumption that the local water movement can be treated as only a translation of quasi-solid plane (e.g., ignoring deformation and rotation in speed fields). This assumption is generally valid over short distances, at least for the features of ocean motion, characterized by a large scale comparatively to the resolution of observations.

The selection of the sizes of the target and search windows in the images depends upon several factors. The size of the target window cannot be so large as to negate this solid-plane assumption, but at the same time, the window size must be large enough so that the comparison for a target area still has some statistical significance. Also, the size of the search window is dependent on the expected water displacement. Because we are talking about small areas of relatively slow movement, the search window could be of a very limited size.

3.4.1 Physics of the Problem

This section discusses the theory behind the problem of estimating ocean flow from difference in sequential satellite imagery. The ODPa is designed to use derived SST fields or ABI infrared observations in order to extract the most accurate water motion.

The motion of water is governed by the balance of acting forces. This can be expressed using what is often called the momentum equation, but is simply Newton's third law of motion:

$$\sum F = ma = m \frac{Du}{Dt}$$

The external stresses acting on ocean surface are the wind stress, τ_a , the water stress, τ_w , the apparent force due to Coriolis, τ_c , the force due the tilt of the water surface τ_t . Therefore,

$$m \frac{Du}{Dt} = \tau_a + \tau_w + \tau_c + \tau_t$$

the relative contribution of the forces is irrelevant, but their spatial inhomogeneities is critically important because spatial changes in surface ocean motion are associated with spatial changes in acting forces.

In most cases, the wind stress at the ocean surface is smoothly changed except in rare cases of very pronounced fronts. The influence of Coriolis force at the ocean surface is secondary. The spatial changes in the water stress and the force due to ocean surface tilt depend on a scale of ocean eddies and other inhomogeneities.

The obvious conclusion that spatial changes in water speed are associated with spatial changes in external forces allows one to estimate the limits of conditions where the main assumption about local quasi-solid plane water movement is applicable and simply conclude that proposed methodology describes ocean motion with a characteristic scale larger than the target size. Thus the results of ODPA are applicable to analyze processes of a spatial scale only above a certain threshold.

Ocean motion is determined through the tracking features of ocean surface properties in time. Identifying features to be tracked is the first step in the process. These features can be inhomogeneous in brightness temperature or SST.

The choice of the spectral band will determine the intended target on the ocean surface to be tracked. Longwave infrared (LWIR) channels could be used for deriving vectors any time of day. During night-time imaging periods, the shortwave (3.9um) infrared (SWIR) channel could compliment the LWIR channel to derive ocean motion. The SWIR channel is a slightly “cleaner” window channel than the LWIR (less attenuation by water vapor), making it more sensitive to warmer surface temperature features (*Dunjon and Velden, 2002*). The SWIR channel is also not as sensitive as the LWIR channel to thin cirrus clouds that may partially obscure surface temperature features. These two characteristics make it a potentially superior channel for identifying and tracking surface temperature targets at night.

As described previously, the size of each target tracked in time is a function of both the spatial and temporal resolution of the imagery and the scale of the intended feature to be tracked. Generally speaking, a small target box yields a noisier motion field than one generated with a

larger target box. Conversely, if the target scene is too large, the algorithm will tend to measure the mean flow of the pixels in the target scene (i.e. a spatial average of several motions) rather than the intended instantaneous motion at a central target point. These considerations need to be kept in mind when choosing the optimal target box size.

3.4.1.1 Target Selection

The objectives of the target selection process are to select high quality target scenes that capture the intended targets (cloud-free area with SST or brightness temperature gradients) and contain sufficient contrast. Targets that possess these characteristics are amenable to more precise tracking that should result in more accurate ocean motion estimates.

Target scenes are re-centered at pixel locations where the magnitude of the brightness temperature gradient is the largest. In other words, these target scenes are centered over brightness temperature of SST gradients in cloud-free areas. A high degree of uniformity usually corresponds to the regions that are cloud-free that complicates the task of estimating target displacements. Although there are physical reasons for regions of strong temperature gradient to be more prone to cloud formation, the problem is compounded by the tendency of some cloud detection algorithms (particularly those employing a local spatial coherence criterion) to misidentify high gradient features as cloud.

3.4.1.2 Feature Tracking

Feature tracking involves coherent tracking of ocean surface features in the image sequence over a specified time interval. A key assumption made in this process is that the features could be considered as tracers that move with the water flow. Of course, it is understood that water tracers are not necessarily passive. There may be changes in temperatures because of thermodynamic and other processes. Therefore it is important to apply robust quality control to remove retrieved vectors that are erroneous as a result of these complicating factors.

The evolution of targeted features depends on many factors including their size and location. To be effectively tracked, tracers should undergo relatively small changes in their inhomogeneities for the time interval of the image sequence used. The resolution of the imagery is also an important consideration when tracking features in satellite imagery. *Merill (1989) and Schmetz et al. (1993)* discuss this at length. It is important that the size of the target scene (spatial resolution) is consistent with the temporal resolution of the imagery in order to capture the scale of the intended feature being tracked. For example, in some cases estimation of motion could be improved by using smaller target scenes and higher temporal resolution imagery.

A critical factor to derive water motion is the image registration; that is, the stability of the image-to-image navigation. If the stability of the image-to-image navigation is poor for an image sequence, the result will be added noise to the tracking process and poor quality of retrieval. This is obviously true for small features displacements typical for low current speeds where image registration uncertainties could dominate in the errors of true displacement vectors.

To achieve smaller vector errors for predetermined image registration quality, a larger image separation time is required. If typical water speed is approximately 1/20 of surface wind, than 20 times larger time intervals between images is necessary to provide a quality of water motion retrieval similar to wind derivation. Such proportional increase calls for 3 – 6 hour intervals between consecutive images, that corresponds to requirements specified for ocean speed retrieval.

3.4.2 Mathematical Description

After preprocessing, the brightness temperatures to be retrieved from the GOES ABI, the GOES-R operational SST, and the GOES-R cloud mask algorithm will be used directly as part of the ODAP processing. These fields will have an approximate resolution of 2-km. Utilization of the various ABI wavelengths, SST, and cloud mask algorithms should produce ocean motion retrievals with acceptable accuracy.

The further processing in ODAP approach to derive an individual vector consists of the following general steps considered below:

- Locate and select a suitable target in second image (middle image; time= t_0) of a prescribed image triplet
- Use a pattern matching algorithm to locate the target in the earlier and later image. Track the target backward in time (to first image; time= $t_0-\Delta t$) and forward in time (to third image; time= $t_0+\Delta t$) and compute corresponding displacement vectors. Compute the mean vector displacement from the two displacement vectors and assign this final vectors to time = t_0 .
- Perform quality control procedures on the output to edit out or flag suspect vectors. Compute and append quality indicators to each vector.

3.4.2.1 Target Selection

Targets are selected from the middle image of the image sequence. Each line segment of data from the middle image is divided into smaller, box shaped, sub-regions called targets. In general, the size of the target box could depend on the channel being processed and the scale of the motion being estimated. Although not a requirement, the target box is traditionally a square with sides of equal length (in pixels). Generally speaking a small target box yields a noisier motion field than one generated with a larger target box. Conversely, if the target scene is too large, the algorithm will measure the large-scale flow of the atmosphere instead of the vector at a single point. These considerations need to be kept in mind when choosing the optimal target box size.

Once the target scene has been identified, a search is made for the local maximum brightness temperature gradient. The brightness temperature gradient magnitude for each pixel location inside a target is computed from the following equation.

$$Gradient_{Line.Element} = \sqrt{\sum_{k=-2}^{k=2} \{(W_k)(BT_{Ele+k, Line})\}^2 + \sum_{k=-2}^{k=2} \{(W_k)(BT_{Ele, Line+k})\}^2}$$

where: $W_k = \{1/12, 8/12, 0, -8/12, 1/12\}$; for $k = -2$ to 2

BT is the pixel level channel brightness temperature

After the search is made for the local maximum brightness temperature gradient, the target box is repositioned over the pixel containing the maximum gradient magnitude. The intent of repositioning the target scene at the maximum gradient is to focus the target scene on a strong feature that is expected to be effectively tracked over time. Repositioning of the target scenes can result in an irregular spatial distribution of target scenes, and hence, an irregular spatial distribution of the ocean motion vectors.

All of the potential targets undergo quality control tests to determine if the target is a suitable tracer. If a target fails any one of these tests, the target is determined to be a non-suitable tracer and is flagged.

Earth Edge Test

All pixels within the target scene must have valid earth navigation associated with it. If any pixel within the target scene is determined to be located in space (i.e., off the earth edge), the target fails, and is flagged.

Cloud Cover Test

The cloud mask product associated with each pixel is used to classify the target scene as cloudy or clear. When the intent is to track ocean surface features, any cloudy pixels should not be included in analysis. In other words, every pixel in the target scene must be cloud-free for this target scene to be deemed a suitable target. In addition, the search window must be completely cloud-free in both the $t_0-\Delta t$ and $t_0+\Delta t$ scenes. This ensures that the pattern matching algorithm will not be generating a spurious goodness-of-match metric.

Land Test

All pixels within the target scene must be ocean pixels. If any pixel within the target scene is determined to be land or even coast, the target scene fails, flagged, and is not processed further.

The tests described above are applied twice: initially for each considered target and second time for the targets re-centered over the locations of maximum gradients.

3.4.2.2 Feature Tracking

A target, represented by an $N \times N$ array of pixels, defines a suitable feature in the image whose movement can be tracked in time. The sum of squared differences (SSD) method is used to track ocean surface features in three image sequence from the middle one backwards and forwards in time before an average of the two displacements is taken. The average vector is assigned to the middle image target location.

The sum-of-squared-differences method (SSD) used by the ODAP algorithm minimizes the following sum:

$$\sum_{x,y} [I_1(x, y) - I_2(x, y)]^2$$

where: I_1 is the brightness temperature at pixel (x, y) of the target scene, I_2 is the brightness temperature at pixel (x, y) of the search window, and the summation is performed over two dimensions. In practice, the region over which the search is conducted is substantially larger than the size of the target scene and the above summation is carried out for all target box positions within the search region. The array of positions that the target box can assume in the search region is often referred to as the “lag coefficient” array. Note that the lag coefficient array is a rectangle. Typically the element size (x-axis) of the lag array is slightly larger than the line (y-axis) size in order to capture the motion caused by the naturally dominant zonal currents. A larger element size has also been used in the past to account for oversampling along the scan line for the current series of GOES satellites.

An example of the output of the SSD algorithm applied to Meteosat-8 data is shown in Figure 2. The SSDs are shown for a target at the central epoch time t versus the search window for $t-1$ and $t+1$, thus the location of the minima have thereabouts opposite displacement with respect to the center of the search window.

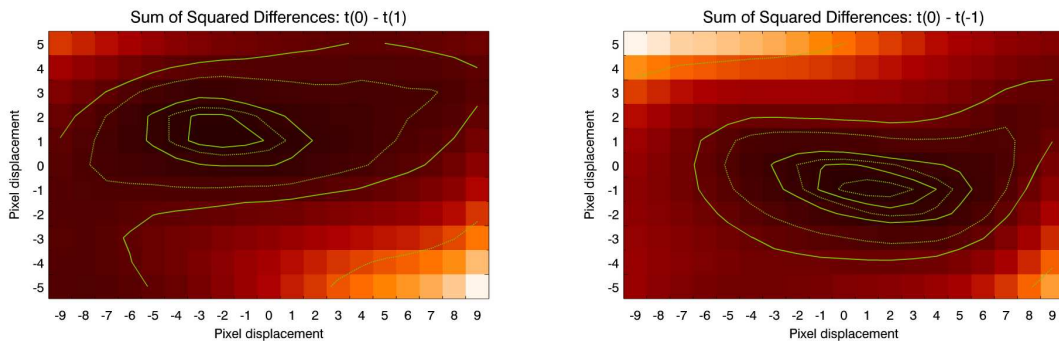


Figure 2: An example of the output of the SSD algorithm applied to Meteosat-8 data

Quality control of the retrieved vectors is performed through the application of several gross error checks aimed at identifying any vectors that are in obvious error.

If either of the intermediate matching scenes derived from the SSD method are found on the boundary of the search scene, then the match scene is flagged. This condition may indicate the true matching solution is located beyond the domain of the search scene.

Correlation Test

The correlation scores of each of the intermediate (i.e., the reverse and forward) matching scenes (derived from the SSD method) are checked to see if they exceed the minimum threshold value of 0.60. If either scene fails this correlation test, the product is flagged as unacceptable in the output file. This is to ensure only highly correlated values for output.

3.5 Algorithm Output

Output from the ODPA consists of the following:

An ASCII file containing a list of parameters for each derived ocean current vector. These parameters include:

- Date (year and Julian day)
- Time (hour)
- Latitude (degrees)
- Longitude (degrees)
- Speed of average ocean vector (m/s)
- Direction of ocean vector (degrees)
- Magnitude on maximum gradient
- u-component of vector 1 (m/s) [backward in time]
- v-component of vector 1 (m/s) [backward in time]
- u-component of vector 2 (m/s) [forward in time]
- v-component of vector 2 (m/s) [forward in time]
- Tracking correlation of vector 1 [backward in time]
- Tracking correlation of vector 2 [forward in time]

The format of the output is identical for both the Ocean Currents and Ocean Currents: Offshore products. The quality of the ODP is defined by the magnitude of the maximum gradient.

3.6 Product Quality

3.6.1 Quality flags

All of the potential targets undergo quality control tests to determine if the target is a suitable and good tracer. There are two groups of tests in target selection: suitability tests and reliability tests. If a target fails any test from the first group, the target is determined to be a non-suitable tracer, its processing stops, motion vectors are not calculated and therefore are not included in output

from calculations. If however, a target fails only reliability tests, the motion vectors are calculated and flagged.

The quality flags are assigned to bit locations in a quality word as shown in Table 5. Any bit set indicates potential for sub-optimal quality.

Quality flag word bit definitions								
Bit location	7 (MSB)	6	5	4	3	2	1	0 (LSB)
Meaning	← Reserved for future use →				Target-to-match correlation < threshold	Sensor zenith angle > threshold	Potential out-of-bounds	Target gradient < threshold

Table 5: Quality flag word bit definitions

3.6.2 Product Quality Information

Since the algorithm does not use any ancillary data and has only one processing path, there is no specific product quality information beyond the quality flags described above.

3.7 Metadata

3.7.1 File Level Metadata summarizing the contents of the data file

Common metadata for all data products

- » DateTime (swath beginning and swath end)
- » Bounding Box
 - product resolution (nominal and/or at nadir)
 - number of rows and
 - number of columns,
 - bytes per pixel
 - data type
 - byte order information
 - location of box relative to nadir (pixel space)
- » Product Name
- » Product Units
- » Ancillary Data to Produce Product (including product precedence and interval between datasets is applicable)
 - Version Number
 - Origin (where it was produced)
 - Name

- » Satellite
- » Instrument
- » Altitude
- » Nadir pixel in the fixed grid
- » Attitude
- » Latitude
- » Longitude
- » Grid Projection
- » Type of Scan
- » Product Version Number
- » Data compression type
- » Location of production
- » Citations to Documents
- » Contact Information

3.7.2 Product specific metadata for Ocean Dynamics (separately for oceans and offshore oceans)

- » Band number 14 (9)
- » Target box size being tracked
- » Date & Time of prior image
- » Date & Time of subsequent image
- » Geographic bounding box
- » Min, Max, Mean and Stddev of reflectance/radiance/brightness temperature
- » Number of suitable targets for calculations
- » Number of cloud free targets
- » Number of good targets for calculations
- » Total number of vectors calculated
- » Mean, Min, Max and stddev for U component
- » Mean, Min, Max and stddev for V component
- » Mean observation-calculations for U component
- » Mean observation-calculations for V component
- » Standard deviation between observation-calculations for U component
- » Standard deviation between observation-calculations for U component
- » Number of quality flags and their definitions
- » Number of retrievals for each quality flag

4 TEST DATA SETS AND OUTPUTS

The SSDs are shown for a target at the central epoch time t versus the search window for $t-1$ and $t+1$, thus the location of the minima have thereabouts opposite displacement with respect to the center of the search window.

4.1 GOES-R Proxy Input Data Sets

The data used to test the ODPA currently include SEVIRI data and validation of ODPA, as it is the best ABI proxy in terms of spectral and temporal features.

4.1.1 SEVIRI Data

In terms of the ABI proxy data, the Spinning Enhanced Visible and Infra-red Imager (SEVIRI) instrument onboard the European Meteosat Second Generation (MSG) satellite (*Schmetz et al, 2002*) is being used since it is the best surrogate system for the future ABI. The spectral coverage and pixel level resolution of the SEVIRI instrument are fairly similar to those expected from the ABI instrument, as is the noise level of the various channels. Furthermore, the navigation and registration performance of the SEVIRI instrument is comparable to the expected ABI instrument performance. Finally, the scanning rate of the SEVIRI instrument is similar to the nominal scanning strategies for the ABI instrument. Table 6 below lists the SEVIRI band that is used in ODPA development and validation pre-launch phase activities. For reference, the corresponding ABI channel is also listed in this table.

SEVIRI				ABI		
Band Number	Wavelength Range(μm)	Central Wavelength (μm)	Sensor Noise	Band Number	Wavelength Range (μm)	Central Wavelength (μm)
9	9.80 - 11.80	10.80	0.13 K @ 300K	14	10.80 – 11.60	11.20

Table 6: SEVIRI channels serving as GOES-R ABI proxy data for the GOES-R ODAP

SEVIRI datasets being used for ODAP product development and validation activities include full-disk Meteosat-8 SEVIRI data from four months of 2005. Use of the full-disk SEVIRI observations enables an analysis of the ODAP over a full range of conditions. Figure 3 shows a sample of full-disk SEVIRI image.

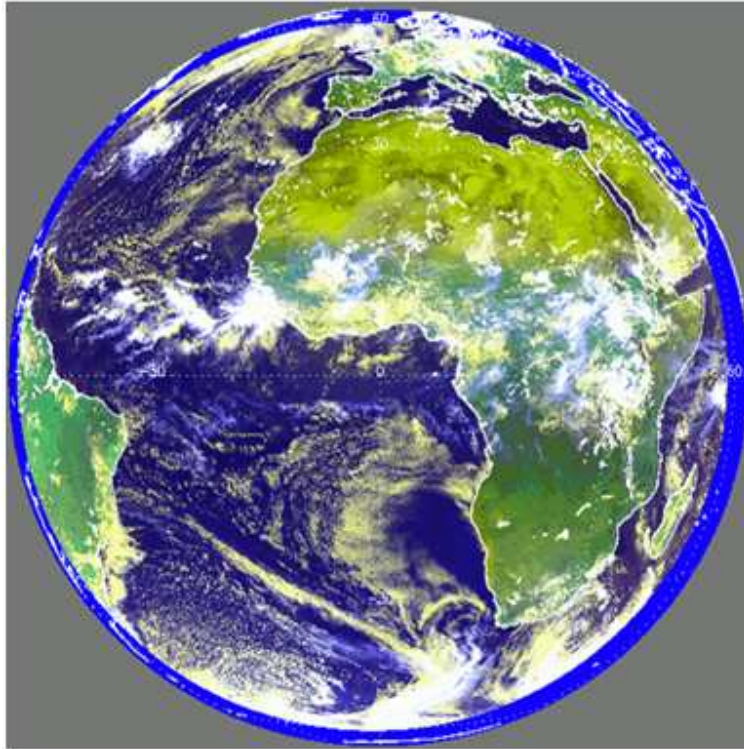


Figure 3: Full disk 0.63, 0.86 and 11 μm false color image from SEVIRI for 2 UTC on 4 Aug 2006

4.2 Output from Proxy Data Sets

4.2.1 SEVIRI Brightness Temperatures

An example of vectors obtained from the ocean dynamics algorithm for July 8, 2005 is shown in Figure 4. All test scenes are centered around $t(0) = 12$ UTC, with $t(-1)$ and $t(+1)$ being 09 UTC and 15 UTC respectively. In this case, the strong upwelling off the coast of N. Africa results in a complex pattern in the region of the Canary Islands.

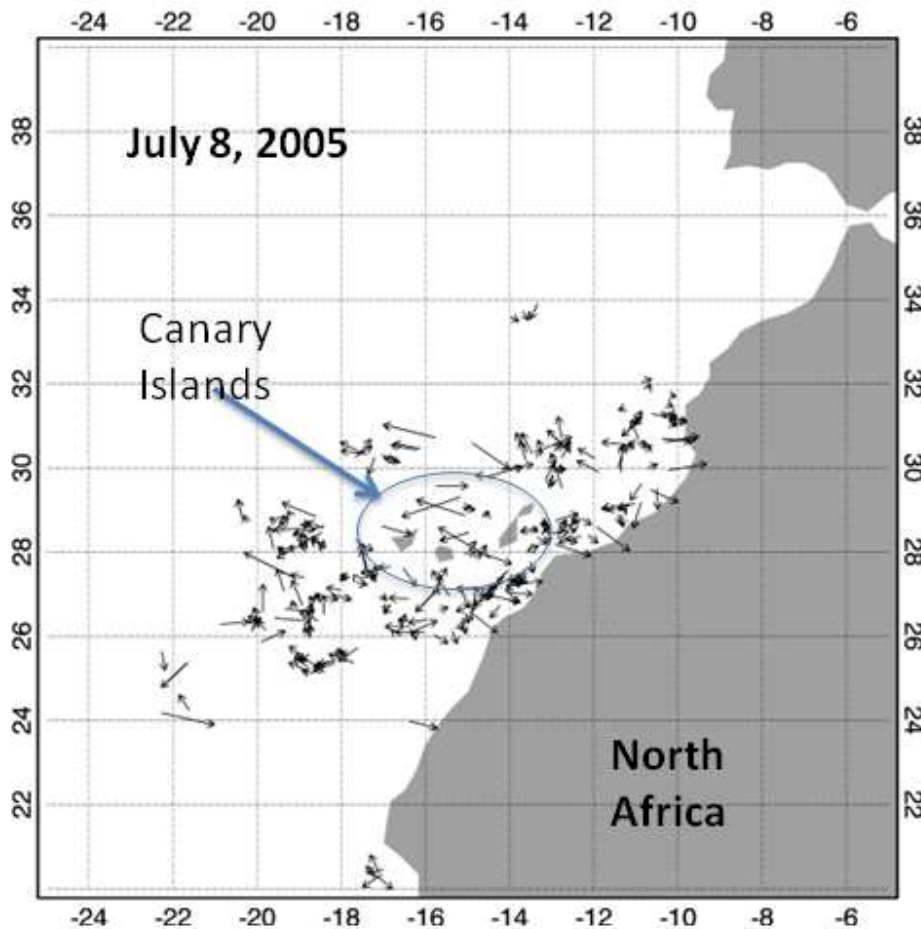


Figure 4: Example vector output from Ocean Dynamic Algorithm derived from Meteosat-8 SEVIRI image triplet centered at 12 UTC on July 8, 2005

4.3 Precision and Accuracy Estimates

This section describes the performance and product quality of the ODAP relative to the specifications found within the GOES-R Functional and Performance Specification Document (F&PS). To estimate the precision and accuracy of the DMW product requires coincident measurements of reference (“truth”) ocean vectors for multiple seasons. The reference (“truth”) datasets used include ocean vectors provided by an oceanographic model (NCOM). The NCOM analysis current fields are used to determine the performance of the ODAP product over oceanic regions. Here, the analysis currents are collocated with ocean vector retrieved from SEVIRI information for the same time of observations. An advantage of this approach is that the collocation match can be generated for every vector produced.

The accuracy and precision estimates for the ODAP products are determined by computing the Mean Difference (MVD) and Standard Deviation (SD) metrics for vector components. The mean difference between retrieved and reference (“truth”) components represents the *accuracy* (*average error*) of the GOES-R ABI ODAP product.

The Standard Deviation (SD) about the mean vector difference between the retrieved GOES-R ABI ODAP product and the reference wind data represents *the precision* (*random error*) of the ABI ODAP product.

The GOES-R ABI ODAP products are considered validated and corresponding to accuracy and precision satisfying the 80% requirements specified within the F&PS document.

4.3.1 Validation against NCOM

Since the primary proxy dataset is Meteosat-8 SEVIRI, the lack of coincidence between readily-accessible CODAR data and the satellite imagery constrains the validation somewhat. Current vectors from global version of the US Navy NCOM (Navy Coastal Ocean Model) are compared with the output of the Ocean Dynamics Algorithm as an initial validation. Figure 5 shows example output of the NCOM. As can be seen, the current vector fields are quite smooth and are at a resolution of $1/8^\circ$, which should be sufficient to be eddy-resolving as the Rossby Radius of deformation is ~ 20 km at mid-latitudes.

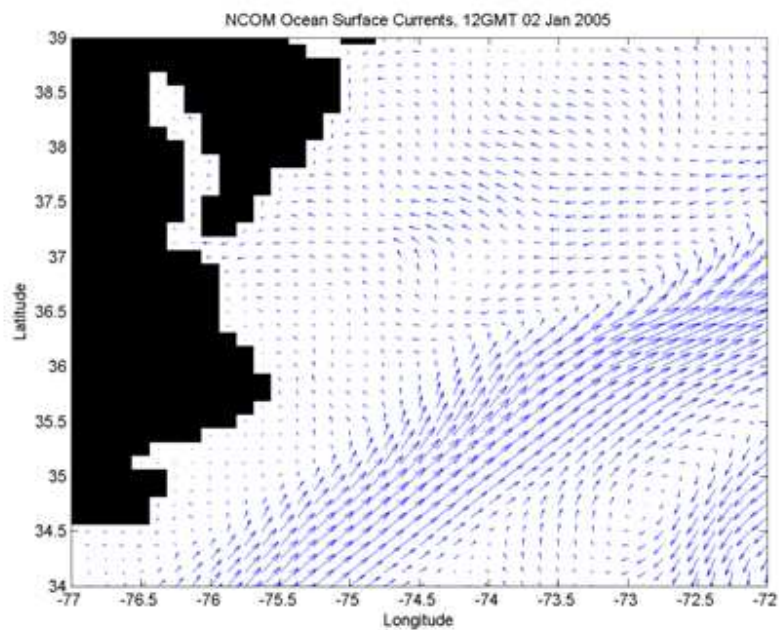


Figure 5: An example of the output from the US Navy NCOM Model

The distributions of ODA – NCOM vector component differences are shown in Figure 6, along with Gaussian curves corresponding to the standard deviation (orange curve) and

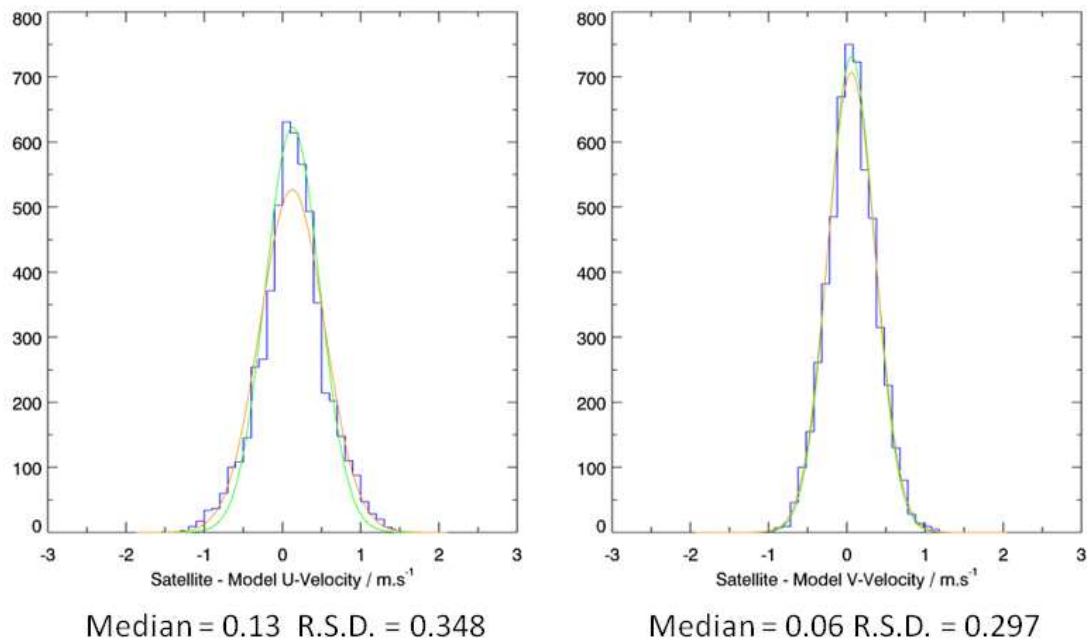


Figure 6: The distribution of the Ocean Dynamics Algorithm-NCOM vector component differences.

inter-quartile range (75th percentile - 25th percentile, green curve). Note that the peak of the distribution is better represented by the Gaussian derived from the inter-quartile range, especially for the U-component. The geographical distribution of the vector component differences are shown in Error! Reference source not found.. Note that large differences in U-component are more prevalent in certain regions, while V-component differences display little geographical preference.

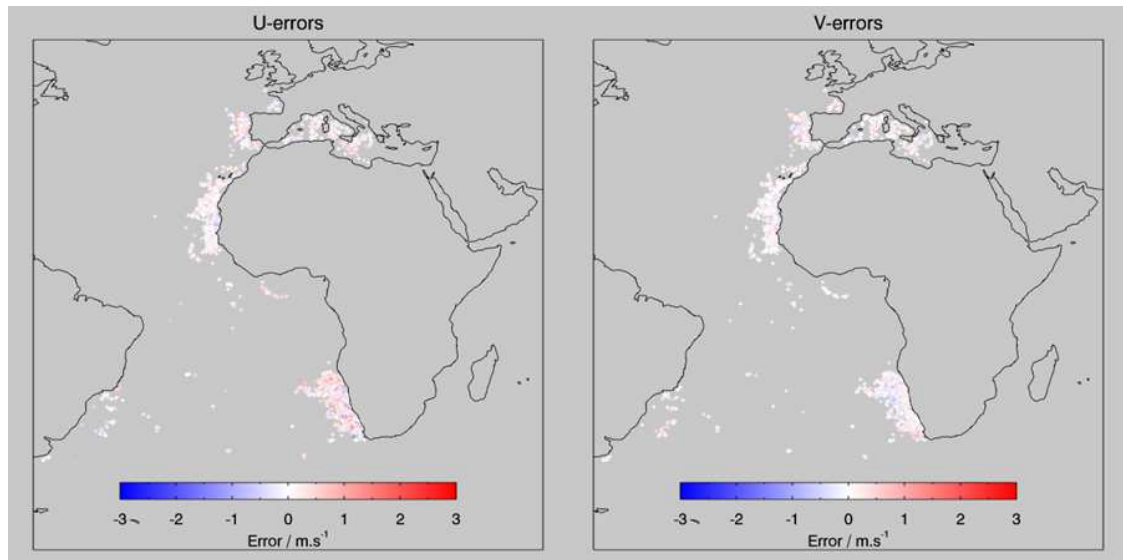


Figure 7: The geographical distribution of the vector component differences.

Figure 8 illustrates the relationship between strength of gradient within target window and vector component difference. As can be seen, targets with weaker gradients tend to have larger discrepancies between ODA and NCOM vector components. If gradient strengths weaker than 0.3 are excluded, the RMS of vector component differences meet 100% of specification (0.3 m.s-1) for the V-component and 80% of specification for the U-component. It is necessary to increase the gradient cutoff to ~0.5 in order for the U-component to meet specification at the 100% level. A summary of the variation in vector component differences by season is shown in Table 7. Note that, although the results do display inter-seasonal variation, and that the U-component does not currently meet 80% of specification for summer, these statistics have been derived from a relatively limited sample (one image triplet centered at 12 UTC for 8 consecutive days in each season).



Figure 8: Illustrates the relationship between strength of the gradient within the target window and the vector component difference.

PERCENTAGE OF REQUIREMENTS MET							
GREEN= 100%		YELLOW=80%		RED= 50%			
SEASON	Mean U	S.D. U	Mean V	S.D. V	%<0.375	%<0.375	
WINTER	-0.1002	0.2218	-0.0330	0.2125	90.44	92.43	
SPRING	-0.2448	0.3452	-0.0286	0.2953	76.27	83.05	
SUMMER	-0.0518	0.4371	0.0352	0.2781	58.90	80.82	
AUTUMN	-0.1795	0.3270	-0.0770	0.3414	77.52	70.54	
YEAR	-0.1299	0.3078	-0.0339	0.2706	79.49	83.98	

Table 7: Seasonal variation of retrieval accuracy for vectors derived from well-defined features

5 PRACTICAL CONSIDERATIONS

5.1 Numerical Computation Considerations

The pattern matching performed by the ODAP is the most computationally intensive aspect of the entire derivation process. It is natural then to focus on this step when considering ways to improve the overall performance of the algorithm.

Current realization of the algorithm saves resources not processing the second pair in image triplets if vector retrieved from the first pair is considered unreliable. Another planned efficiency upgrades (that could result in a 25% improvement in the processing times) is to terminate the sum-of-squared differences (SSD) calculation early once a current minimum value has been exceeded. The rationale for terminating the summation early is obvious as any additional calculations would simply increase the summation value above the current minimum.

But the most significant resource to increase efficiency of processing in ODAP is to remove any relationships in codes to cloud height. The largest part of this task is already realized, but some additional efforts will be required to remove unneeded calculations in preprocessing.

5.2 Programming and Procedural Considerations

The current version of the ODAP includes a data buffer that holds information (radiance, brightness temperature, cloud mask, etc) from adjacent line segments (also called swaths). Such a buffer makes it possible for the algorithm to track features that move out of the domain of the middle line segment, which is the only part of the buffer being processed for targets. With each new line segment read in, data in the buffer is shifted upwards so that the “oldest” data is always at the top of the buffer while the new segment data is added to the bottom of the buffer. This involves a substantial amount of copying from one segment of the buffer to another. It is anticipated that future versions of the algorithm will not have this buffer, as it is expected that the processing framework provided by the Algorithm Integration Team (AIT) will take care of this task. This will greatly simplify the algorithm and should significantly improve its performance.

Currently, output from the DMWA consists of an ASCII file containing a limited number of parameters. It should be emphasized that this ASCII file was created for testing purposes only. It is recognized that a common IO interface (i.e., netCDF format) will need to be incorporated into the algorithm. This issue will be addressed when the AIT provides the Algorithm Working Group (AWG) teams with the necessary routines.

5.3 Quality Assessment and Diagnostics

The following procedures are recommended for diagnosing the performance of this algorithm.

- Monitor the products with “truth” including *in situ* observations.
- Map the spatial distribution of calculated vectors to look for artifacts or non-physical behaviors.

Code checkers provided by the AIT will be used to assess compliance with the AIT coding standards. If programs are provided to diagnose the efficiency of the code, these will be used as well.

5.3.1 Exception Handling

Exception handling is required for the development of robust and efficient software realization. Requirements set forth by the AIT also stress the importance of exception handling. While the main modules of the ODAP program (`target_selection.f90` and `feature_tracking_utils.f90`) will use the AIT-provided subroutine for error messaging, its use is limited. More extensive error checking will be added to future versions of the ODAP.

For the most part, the ODAP assumes that all necessary images and ancillary data are available through the processing framework. The only data that the algorithm explicitly checks for is the temporal brightness temperature data, which is necessary for the tracking portion of the algorithm. If the temporal data is unavailable, the algorithm outputs an error message and control is returned to the processing framework.

As part of the target selection process, the ODAP checks for missing or unrealistic values within both the target and search regions. If either condition is met, the algorithm will flag the scene as bad and proceed to the next adjacent scene.

5.3.2 Validation

Validation of the ODAP products requires collocated measurements of reference (“truth”) vector values for the full range of ABI observing geometry and environmental conditions. From these collocated measurements, comparison metrics that characterize the agreement between the satellite-derived motion vectors and the reference values are calculated.

5.3.2.1 Proposed Alternative Validation Sources

The validation of the ODAP Product will be based upon various testing data sets, each with its own strengths and weakness. As with most oceanographic products, in-situ datasets provide a consistent, although spatially sparse, form of comparison. Data from worldwide drifter buoy deployment could be integrated into the validation. However, these velocities will not necessarily provide an accurate depiction of the surface current. Data from ocean moorings, such as provided by the TAO/TRITON/PIRATA arrays, provide ocean current time series at various depths, including near-surface measurements.

Ocean model fields, such as the *Real-Time Ocean Forecast System (RTOFS)* provide surface and subsurface parameters that will allow for the testing and validation of the OD algorithm. Typically, the temporal and spatial resolution of such models is not as fine as that which GOES-R will provide, and may not necessarily correctly address the physical oceanographic dynamics. For example, in the case of RTOFS, the location of the Gulf Stream is often translated approximately 200 km to the south of its actual position (Figure 9).

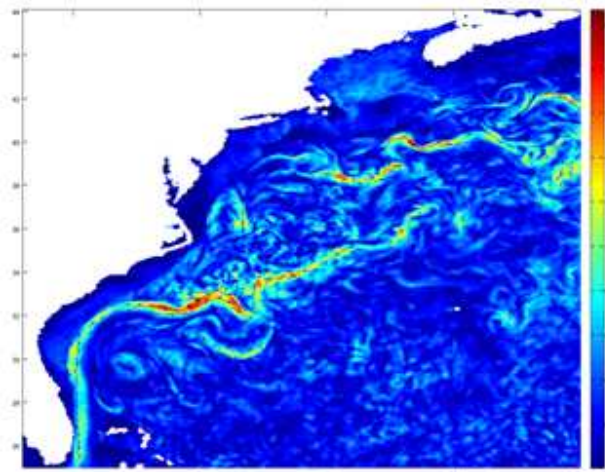


Figure 9: Surface Current Field of the Northwest Atlantic from Real-Time Ocean Forecast System. Note the erroneous position of the core of the Gulf Stream.

Another dataset intended to validate motion vectors is *Ocean Surface Current Analyses – Real time (OSCAR)*. This NOAA/NESDIS dataset derives surface currents from satellite altimeter and scatterometer data, providing world wide data at 100 km resolution. This extremely coarse spatial resolution (when compared to GOES-R), along with data limitations near the coast (Figure 10) and the temporal resolution (on the order of 5 days) may only allow a very general statistical comparison.

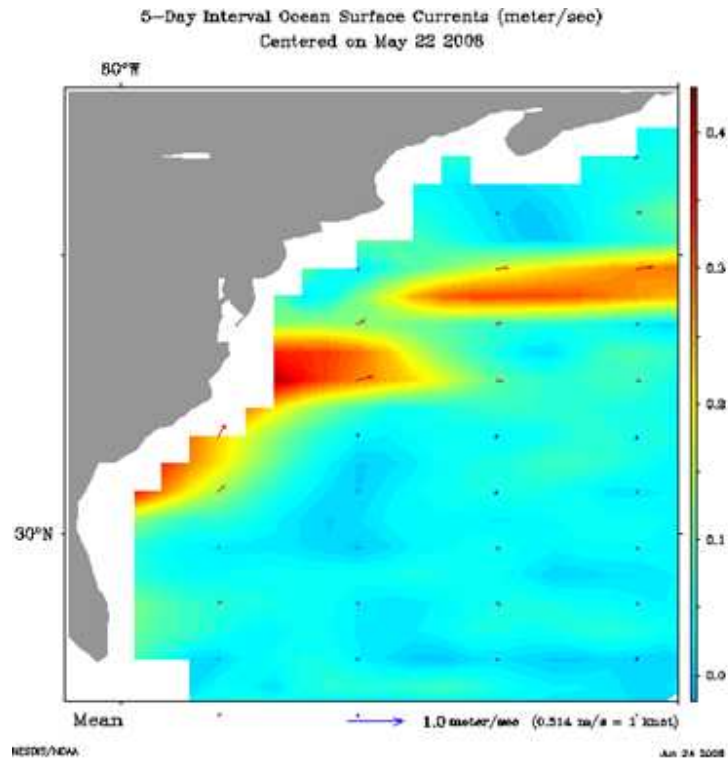


Figure 10: Example of the surface current field from the Ocean Surface current Analyses-Real time, available from NOAA/NESDIS. Note the coarse spatial resolution, and the inability to derive currents within 100 km of the coastline.

Figure 11 presents an example of ocean surface currents from CODAR in near-coastal zone. These data have comparable spatial resolution to GOES-R, and are updated in near real-time at many locations along the coast of the continental US, particularly off the coast of California, Oregon and Washington, as well as the Mid-Atlantic Bight. CODAR uses a transmitter to send out a radio frequency that scatters off the ocean surface and back to a receiver antenna. While this data is highly desirable for the testing and validation of GOES-R OSC due to its temporal and spatial resolution, comparisons are limited to the coastal zone, perhaps extending out as far as the continental shelf-break.

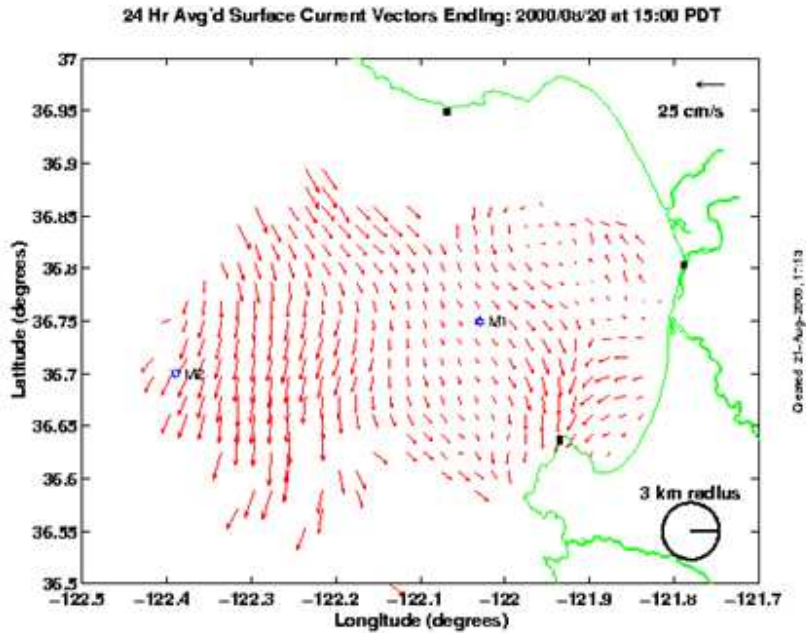


Figure 11: Example of ocean surface currents from CODAR off of California

During the pre-launch phase of the GOES-R program, the product validation activities are aimed at characterizing the performance and uncertainties of the ODAP products resulting from parameterizations and algorithmic implementation artifacts. During this phase, there is total reliance on the use of GOES-R ABI proxy and simulated datasets. Post-launch validation will apply lessons learned to inter-comparisons of actual operational products generated from real ABI measurements and reference (“ground-truth”) observations. Validation methodologies and tools developed and tested during the pre-launch phase will be automated and applied.

6 ASSUMPTIONS AND LIMITATIONS

The following sections describe the current limitations and assumptions in the current version of the ODAP.

6.1 Performance

The following assumptions have been made in developing and estimating the performance of the ODAP.

1. The ACM provides an accurate clear sky mask for the current, previous, and future images in a timely manner.
2. Land mask maps are available to identify land/water pixels and is available at pixel resolution

3. Pixel level sensor data for used channels are available for all three images in the sequence along with accompanying meta-data (latitude, longitude, image scan times, and quality flags).
4. All data is in the same gridded format and in the same orientation.

6.2 Assumed Sensor Performance

We assume the sensor will meet its current specifications. However, the ODAP will be dependent on the following instrumental characteristics.

- Data retrieval will be critically dependent on the amount of striping in the data.
- The ODAP is critically dependent on the ACM as well as 11 micron sensor data.
- Errors in navigation from image to image will significantly contribute to the quality of motion vector calculations.
- All sensor issues can play a role in accurate clear sky detection. In addition, it is assumed that the ACM is an accurate portrayal of clear/cloudy pixels. Documentation of the ACM is provided in the ACM ATBD.

6.3 Pre-Planned Product Improvements

The quality control indicators attached to each vector are important to the users of these products. Proper interpretation and application of these quality control indicators helps the user community make optimal use of the products. As such, improving these quality control indicators so that they more accurately represent the integrity and accuracy of the product is vital.

The possible product improvements will depend on modifications of the developed approach and algorithm realizations.

7 REFERENCES

Breaker, L.C, T. P. Mavor and W. W. Broenkow, 2005: Mapping and monitoring large-scale ocean fronts off the California Coast using imagery from GOES-10 geostationary satellite. Publ. T-056, 25 pp, *California Sea Grant College Program*.

Castelao, R. M., T. P. Mavor, J. A. Barth and L. C. Breaker, 2006: Sea-surface temperature fronts in the California Current System from geostationary satellite observations. *Jour. Geophys. Res.*, **111**

Castelao, R. M., J. A. Barth and T. P. Mavor, 2005: Flow-topography interactions in the northern California Current System observed from geostationary satellite data. *Geophys. Res. Letters*, **32**.

Dunion, J. P., and C. S. Velden, 2002: Application of surface-adjusted GOES low-level cloud-drift winds in the environment of Atlantic tropical cyclones. Part I: Methodology and validation. *Monthly Weather Review*, 130, 1333-1346.

Merrill, R.T., 1989: Advances in the automated production of wind estimates from geostationary satellite imagery. Preprints, *Fourth Conf. on Satellite Meteorology and Oceanography*, San Diego, CA, Amer. Meteor. Soc., 246–249.

Merrill, R.T., W. P. Menzel, W. Baker, J. Lynch, and E. Legg, 1991: A report on the recent demonstration of NOAA's upgraded capability to derive cloud motion satellite winds. *Bull. Amer. Meteor. Soc.*, **72**, 372–376.

Nieman, S.J., J. Schmetz, and W.P. Menzel, 1993: A comparison of several techniques to assign heights to cloud tracers. *J. Appl. Meteor.*, **32**, 1559–1568.

Schmetz J., K. Holmlund, J. Hoffman, B. Strauss, B. Mason, V. Gaertner, A. Koch and L. van de Berg, 1993: Operational cloud motion winds from Meteosat infrared images, *J. Appl. Met.*, **32**, 1206-1225.

T. J. Schmit, M. M. Gunshor, W. Paul Menzel, Jun Li, Scott Bachmeier, James J. Gurka, 2005: Introducing the Next-generation Advanced Baseline Imager (ABI) on GOES-R, *Bull. Amer. Meteor. Soc.*, Vol. 8, pp. 1079-1096.

Velden, C., J. Daniels, D. Stettner, D. Santek, J. Key, J. Dunion, K. Holmlund, G. Dengel, W. Bresky, W.P. Menzel, 2005: Recent innovations in deriving tropospheric winds from meteorological satellites. *Bull. Amer. Meteor. Soc.*, **86**, 205-221.

Velden, C., D. Stettner, and J. Daniels, 2000: Wind vector fields derived from GOES rapid-scan imagery. *Proc. 10th Conf. on Satellite Meteor. and Oceanogr.*, Long Beach California, Amer. Meteor. Soc., 20–23